Article

Electrospray Ionization Mass Spectrometry of Uniform and Mixed Monolayer Nanoparticles: Au[S(CH)Ph] and Au[S(CH)Ph](SR)

Joseph B. Tracy, Matthew C. Crowe, Joseph F. Parker, Oliver Hampe, Christina A. Fields-Zinna, Amala Dass, and Royce W. Murray

J. Am. Chem. Soc., **2007**, 129 (51), 16209-16215 • DOI: 10.1021/ja076621a

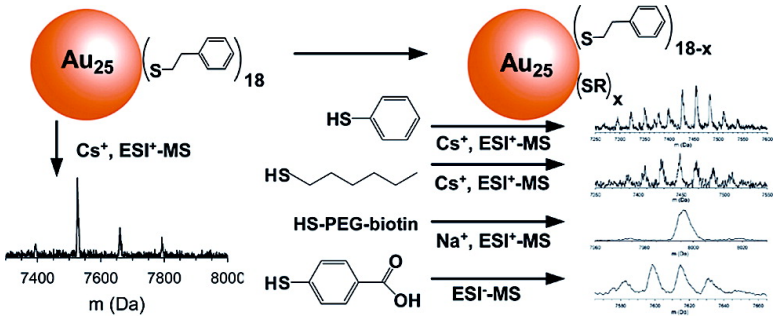

More About This Article

Additional resources and features associated with this article are available within the HTML version:

- Supporting Information
- Links to the 19 articles that cite this article, as of the time of this article download
- Access to high resolution figures
- Links to articles and content related to this article
- Copyright permission to reproduce figures and/or text from this article

View the Full Text HTML

J|A|C|S
ARTICLES
Published on Web 11/23/2007

Electrospray Ionization Mass Spectrometry of Uniform and Mixed Monolayer Nanoparticles: $Au_{25}[S(CH_2)_2Ph]_{18}$ and $Au_{25}[S(CH_2)_2Ph]_{18-x}(SR)_x$

Joseph B. Tracy,[†,§] Matthew C. Crowe,[†] Joseph F. Parker,[†] Oliver Hampe,[‡] Christina A. Fields-Zinna,[†] Amala Dass,[†] and Royce W. Murray*[,†]

Contribution from the Kenan Laboratories of Chemistry, University of North Carolina, Chapel Hill, North Carolina 27599, and Institute for Nanotechnology, Forschungszentrum Karlsruhe, 76021 Karlsruhe, Germany

Received September 3, 2007; E-mail: rwm@email.unc.edu

Abstract: New approaches to electrospray ionization mass spectrometry (ESI-MS)—with exact compositional assignments—of small (Au_{25}) nanoparticles with uniform and mixed protecting organothiolate monolayers are described. The results expand the scope of analysis and reveal a rich chemistry of ionization behavior. ESI-MS of solutions of phenylethanethiolate monolayer-protected gold clusters (MPCs), $Au_{25}(SC2Ph)_{18}$, containing alkali metal acetate salts (MOAc) produce spectra in which, for Na^+, K^+, Rb^+, and Cs^+ acetates, the dominant species are $MAu_{25}(SC2Ph)_{18}^{2+}$ and $M_2Au_{25}(SC2Ph)_{18}^{2+}$. Li^+ acetates caused ligand loss. This method was extended to the analysis of Au_{25} MPCs with mixed monolayers, where thiophenolate (−SPh), hexanethiolate (−SC6), or biotinylated (−S−PEG−biotin) ligands had been introduced by ligand exchange. In negative-mode ESI-MS, no added reagents were needed in order to observe $Au_{25}(SC2Ph)_{18}^-$ and to analyze mixed monolayer Au_{25} MPCs prepared by ligand exchange with 4-mercaptobenzoic acid, HSPhCOOH, which gave spectra through deprotonation of the carboxylic acids. Adducts of tetraoctylammonium (Oct_4N^+) with $-SPhCOO^-$ sites were also observed. Mass spectrometry is the only method that has demonstrated capacity for measuring the exact distribution of ligand-exchange products. The possible origins of the different Au_{25} core charges (1−, 0, 1+, 2+) observed during electrospray ionization are discussed.

Introduction

Monolayer-protected clusters (MPCs) are nanoparticles composed of inorganic cores with monolayer shells of organic ligands whose potential for scientifically novel and technologically useful chemical and physical properties has spurred much interest within the chemistry, electronics, biology, and medical communities. Their potential relies on an ability to determine, ultimately at a substantial level of detail, the composition and structure of MPC nanomaterials. This report on electrospray ionization mass spectrometry[1] (ESI-MS) of small gold MPCs demonstrates the effectiveness of ESI-MS as an analytical technique for obtaining mass spectra of MPCs with intact cores and unfragmented organothiolate ligand shells, both uniform and mixed,[2−4] using an MPC, $Au_{25}(ligand)_{18}$, that has experienced a number of recent investigations.[5−14] ESI-MS is successful for this MPC because it is a soft ionization technique and can provide the MPC composition with atomic precision;[11] what is required is an understanding of the chemistry allowing ionization.

Functionalized MPCs typically have mixtures of ligands in their protecting monolayers. They are useful in fundamental studies and technological applications; the ligands affect nanoparticle solubility and hydrodynamic size and allow incorporation of electroactive or paramagnetic tags, chromophores, or

[†] University of North Carolina.
[‡] Forschungszentrum Karlsruhe.
[§] Current address: Department of Materials Science and Engineering, North Carolina State University, Raleigh, North Carolina 27695.

(1) (a) Dole, M.; Mack, L. L.; Hines, R. L. *J. Chem. Phys.* **1968**, *49*, 2240. (b) Yamashita, M.; Fenn, J. B. *J. Phys. Chem.* **1984**, *88*, 4451.
(2) Hostetler, M. J.; Templeton, A. C.; Murray, R. W. *Langmuir* **1999**, *15*, 3782.
(3) (a) Jackson, A. M.; Myerson, J. W.; Stellacci, F. *Nat. Mater.* **2004**, *3*, 330. (b) Jackson, A. M.; Hu, Y.; Silva, P. J.; Stellacci, F. *J. Am. Chem. Soc.* **2006**, *128*, 11135. (c) Centrone, A.; Hu, Y.; Jackson, A. M.; Zerbi, G.; Stellacci, F. *Small* **2007**, *3*, 814.
(4) DeVries, G. A.; Brunnbauer, M.; Hu, Y.; Jackson, A. M.; Long, B.; Neltner, B. T.; Uzun, O.; Wunsch, B. H.; Stellacci, F. *Science* **2007**, *315*, 358.
(5) Shichibu, Y.; Negishi, Y.; Tsukuda, T.; Teranishi, T. *J. Am. Chem. Soc.* **2005**, *127*, 13464.
(6) Shichibu, Y.; Negishi, Y.; Tsunoyama, H.; Kanehara, M.; Teranishi, T.; Tsukuda, T. *Small* **2007**, *3*, 835.
(7) Negishi, Y.; Chaki, N. K.; Shichibu, Y.; Whetten, R. L.; Tsukuda, T. *J. Am. Chem. Soc.* **2007**, *129*, 11322.
(8) Negishi, Y.; Nobusada, K.; Tsukuda, T. *J. Am. Chem. Soc.* **2005**, *127*, 5261.
(9) Negishi, Y.; Takasugi, Y.; Sato, S.; Yao, H.; Kimura, K.; Tsukuda, T. *J. Phys. Chem. B* **2006**, *110*, 12218.
(10) Shichibu, Y.; Negishi, Y.; Watanabe, T.; Chaki, N. K.; Kawaguchi, H.; Tsukuda, T. *J. Phys. Chem. C* **2007**, *111*, 7845.
(11) Tracy, J. B.; Kalyuzhny, G.; Crowe, M. C.; Balasubramanian, R.; Choi, J. P.; Murray, R. W. *J. Am. Chem. Soc.* **2007**, *129*, 6706.
(12) Ikeda, K.; Kobayashi, Y.; Negishi, Y.; Seto, M.; Iwasa, T.; Nobusada, K.; Tsukuda, T.; Kojima, N. *J. Am. Chem. Soc.* **2007**, *129*, 7230.
(13) (a) Iwasa, T.; Nobusada, K. *Chem. Phys. Lett.* **2007**, *441*, 268. (b) Iwasa, T.; Nobusada, K. *J. Phys. Chem. C* **2007**, *111*, 45.
(14) Negishi, Y.; Tsunoyama, H.; Suzuki, M.; Kawamura, N.; Matsushita, M. M.; Maruyama, K.; Sugawara, T.; Yokoyama, T.; Tsukuda, T. *J. Am. Chem. Soc.* **2006**, *128*, 12034.

biofunctional groups.[5,15−18] Using STM, Au MPCs with mixed monolayers have been shown by Stellacci et al. to exhibit packing patterns on the nanoparticle core surfaces,[3] and this information has been exploited in developing a method for the assembly of covalently linked nanoparticle chains.[4] For many applications, quantitative assessment and control of the mixed-monolayer composition is critical, but there are few analytical techniques for actually measuring other than an *average* of the monolayer compositions over the nanoparticle population, as for example is done in NMR determinations of mixed monolayer compositions.[19] Mass spectrometry is an ideal tool for measuring mixed monolayer compositions because *it alone provides the distribution of ligand exchange products*. The quantity of sample required for ESI-MS analysis (≈50 μg) is also quite small.

High-resolution MPC mass spectrometry also provides information about which core charges are favored in the gas phase. If the total ionic MPC charge and the identity of all bound or dissociated counterions are known, then the core charge can be deduced. These core charges give some insight into the electronic structure and MPC behavior in solution, but the MPC charge in solution is best measured using electrophoresis. In recent work by the C.B. Murray group, electrostatic effects were shown to play an important role in guiding the assembly of binary nanoparticle superlattices, and their observations were rationalized with electrophoretic mobility measurements.[20]

There are three main procedures for preparing mixed-monolayer MPCs: (1) ligand exchange, as performed here,[2] (2) de novo nanoparticle synthesis using multiple ligands,[18] and (3) partial modification of a uniform monolayer after synthesis.[17,19] Ligand exchange is versatile because it generally does not perturb the core size and is applicable to many kinds of ligands and nanoparticle cores. Multiple ligands can be used during the MPC synthesis, but the potential sensitivities of nanoparticle core nucleation and growth to the specific ligands used can lead to unintended changes in nanoparticle size and size distribution. Partial modification of an initially uniform monolayer requires that it have already some functional reactivity, which reduces its generality. ESI-MS analysis of actual mixed ligand distributions produced by these procedures should yield a deeper understanding of how to prepare mixed monolayers having desired compositions.

Following the key development of thiolate-protected Au MPCs by Brust et al.,[21] interest in Au nanoparticles with <5 nm core dimensions has rapidly expanded. Some size-dependent features quickly emerged. MPCs with core diameters $d > \sim 2.0$ nm exhibit a surface plasmon resonance in the visible spectrum at about 520 nm; this feature is damped out at smaller sizes. MPCs with core diameters $\sim 1.5 \text{ nm} < d < \sim 2.5$ nm display quantized double layer (QDL) charging, which corresponds to single electron transfers, in solution voltammetry at room temperature. The smallest ($d < \sim 1.5$ nm) Au MPCs develop a HOMO−LUMO energy gap and are "molecular" rather than metallic.[22] The electronic structure of Au MPCs, and thereby their optical and electrochemical properties, have a strong size dependence and are sensitive to the monolayer composition.[8,9,15,23−25] Methods for accurately measuring both core and monolayer composition are vital to advances in understanding size dependences. A key aim in our ongoing work is to access ESI mass spectra of Au MPCs larger than Au_{25}, which requires additional charging in order to be observed on a mass spectrometer with a limited *m*/*z* range.

The MPC composition $Au_{25}(ligand)_{18}$, where the ligands are thiolates, has been shown to be unusually stable,[6,7] which has been an advantage in recent work on its preparative chemistry and size analysis,[5−11] experimental[12] and theoretical work[13] relating to its structure, and its magnetic properties.[14] An MPC composition originally reported as $Au_{28}(ligand)_{16}$[23,26] has been reassigned[8,11,27] as $Au_{25}(ligand)_{18}$, and on the basis of our recent[11] ESI-MS evidence, phenylethanethiolate (−SC2Ph)-protected Au MPCs initially reported as $Au_{38}(SC2Ph)_{24}$[28] have also been shown to have the composition $Au_{25}(SC2Ph)_{18}$. In our previous ESI-MS study,[11] poly(ethylene glycol) thiolate (S-PEG) ligands were exchanged into the original −SC2Ph monolayer; PEG is known to charge in ESI by coordination to alkali metals,[29] and indeed produced nanoparticle cations. We also observed that the Au core typically carried a 1− charge and additionally saw a spectral peak corresponding to the composition $Na_3Au_{25}(SC2Ph)_{18}^{2+}$, i.e., cation generation without PEG ligands was evidently possible. These observations warranted further study, which has been incorporated in this report that is arranged in four main parts: (1) an in-depth study of $M_nAu_{25}(SC2Ph)_{18}^{2+}$, where M^+ is an alkali metal ion, (2) positive-mode ESI analysis of different kinds of mixed monolayers, (3) negative-mode ESI-MS measurements of $Au_{25}(SC2Ph)_{18}^-$ and of mixed monolayers with carboxylic acids incorporated, which enhance ionization, and (4) a discussion and interpretation

(15) Hostetler, M. J.; Wingate, J. E.; Zhong, C. J.; Harris, J. E.; Vachet, R. W.; Clark, M. R.; Londono, J. D.; Green, S. J.; Stokes, J. J.; Wignall, G. D.; Glish, G. L.; Porter, M. D.; Evans, N. D.; Murray, R. W. *Langmuir* **1998**, *14*, 17.
(16) (a) Levy, R.; Thanh, N. T. K.; Doty, R. C.; Hussain, I.; Nichols, R. J.; Schiffrin, D. J.; Brust, M.; Fernig, D. G. *J. Am. Chem. Soc.* **2004**, *126*, 10076. (b) Hostetler, M. J.; Green, S. J.; Stokes, J. J.; Murray, R. W. *J. Am. Chem. Soc.* **1996**, *118*, 4212. (c) Aguila, A.; Murray, R. W. *Langmuir* **2000**, *16*, 5949. (d) Miles, D. T.; Murray, R. W. *Anal. Chem.* **2001**, *73*, 921. (e) Holm, A. H.; Ceccato, M.; Donkers, R. L.; Fabris, L.; Pace, G.; Maran, F. *Langmuir* **2006**, *22*, 10584. (f) Mirkin, C. A.; Letsinger, R. L.; Mucic, R. C.; Storhoff, J. J. *Nature* **1996**, *382*, 607. (g) Ackerson, C. J.; Jadzinsky, P. D.; Jensen, G. J.; Kornberg, R. D. *J. Am. Chem. Soc.* **2006**, *128*, 2635. (h) Chechik, V.; Wellsted, H. J.; Korte, A.; Gilbert, B. C.; Caldararu, H.; Ionita, P.; Caragheorgheopol, A. *Faraday Discuss.* **2004**, *125*, 279.
(17) Templeton, A. C.; Hostetler, M. J.; Warmoth, E. K.; Chen, S. W.; Hartshorn, C. M.; Krishnamurthy, V. M.; Forbes, M. D. E.; Murray, R. W. *J. Am. Chem. Soc.* **1998**, *120*, 4845.
(18) Ingram, R. S.; Hostetler, M. J.; Murray, R. W. *J. Am. Chem. Soc.* **1997**, *119*, 9175.
(19) Templeton, A. C.; Hostetler, M. J.; Kraft, C. T.; Murray, R. W. *J. Am. Chem. Soc.* **1998**, *120*, 1906.
(20) Shevchenko, E. V.; Talapin, D. V.; Kotov, N. A.; O'Brien, S.; Murray, C. B. *Nature* **2006**, *439*, 55.
(21) Brust, M.; Walker, M.; Bethell, D.; Schiffrin, D. J.; Whyman, R. *J. Chem. Soc., Chem. Commun.* **1994**, 801.
(22) (a) Schmid, G. *Chem. Rev.* **1992**, *92*, 1709. (b) Lee, D.; Donkers, R. L.; Wang, G. L.; Harper, A. S.; Murray, R. W. *J. Am. Chem. Soc.* **2004**, *126*, 6193.
(23) (a) Schaaff, T. G.; Whetten, R. L. *J. Phys. Chem. B* **2000**, *104*, 2630. (b) Negishi, Y.; Takasugi, Y.; Sato, S.; Yao, H.; Kimura, K.; Tsukuda, T. *J. Am. Chem. Soc.* **2004**, *126*, 6518.
(24) Wolfe, R. L.; Balasubramanian, R.; Tracy, J. B.; Murray, R. W. *Langmuir* **2007**, *23*, 2247.
(25) Guo, R.; Murray, R. W. *J. Am. Chem. Soc.* **2005**, *127*, 12140.
(26) (a) Schaaff, T. G.; Knight, G.; Shafigullin, M. N.; Borkman, R. F.; Whetten, R. L. *J. Phys. Chem. B* **1998**, *102*, 10643. (b) Link, S.; Beeby, A.; FitzGerald, S.; El-Sayed, M. A.; Schaaff, T. G.; Whetten, R. L. *J. Phys. Chem. B* **2002**, *106*, 3410.
(27) Wyrwas, R. B.; Alvarez, M. M.; Khoury, J. T.; Price, R. C.; Schaaff, T. G.; Whetten, R. L. *Eur. Phys. J. D* **2007**, *43*, 91.
(28) Donkers, R. L.; Lee, D.; Murray, R. W. *Langmuir* **2004**, *20*, 1945.
(29) (a) Wong, S. F.; Meng, C. K.; Fenn, J. B. *J. Phys. Chem.* **1988**, *92*, 546. (b) Gidden, J.; Wyttenbach, T.; Jackson, A. T.; Scrivens, J. H.; Bowers, M. T. *J. Am. Chem. Soc.* **2000**, *122*, 4692. (c) Wyttenbach, T.; von Helden, G.; Bowers, M. T. *Int. J. Mass Spectrom.* **1997**, *165*, 377. (d) Bogan, M. J.; Agnes, G. R. *J. Am. Soc. Mass Spectrom.* **2002**, *13*, 177.

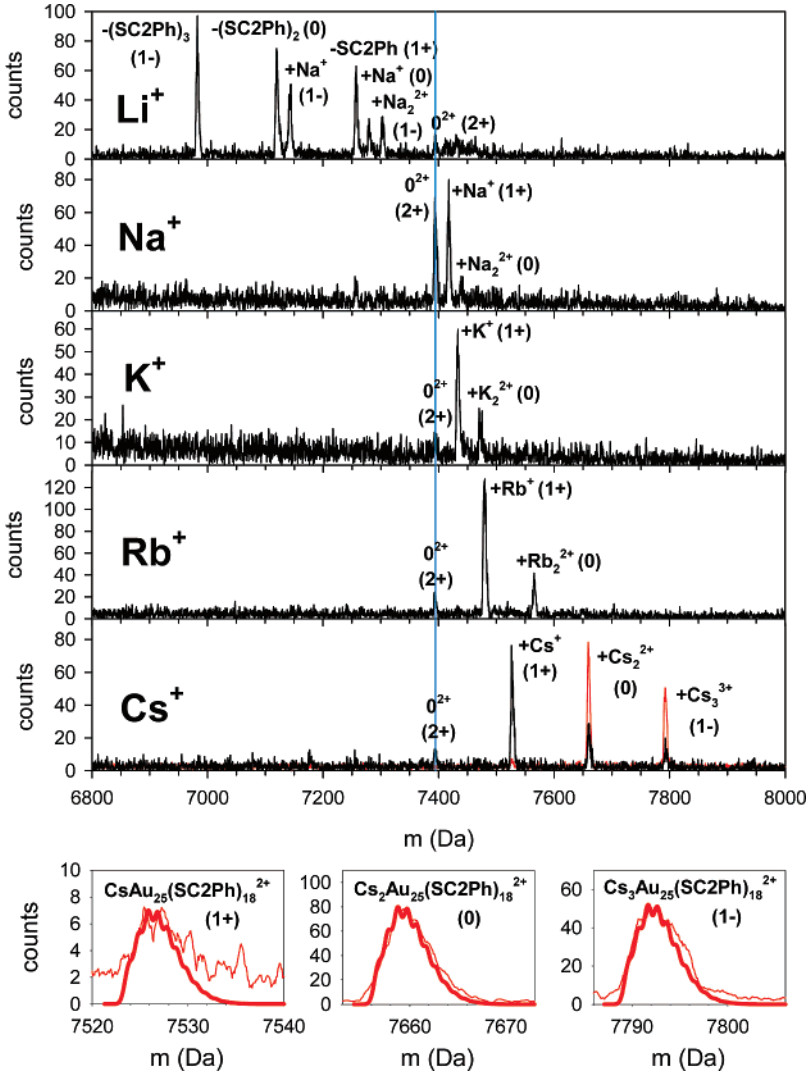

Figure 1. Mass spectra for unexchanged $z = 2+$ ions with labels for M^+ binding, ligand loss, and the core charges in parentheses. The molecular ion, $0^{2+} = Au_{25}(SC2Ph)_{18}^{2+}$. The spectra in black were obtained using 100 mmol MOAc/1 mmol $Au_{25}(SC2Ph)_{18}$ and 30% CH_2Cl_2/70% CH_3OH as the solvent. For LiOAc (top spectrum), no Na^+ was added, but Na^+ binding was observed. For acquisition of the spectrum in red (scaled down by a factor of 0.2), 50 mmol CsOAc/1 mmol $Au_{25}(SC2Ph)_{18}$ was added in 30% toluene/70% CH_3OD. Thick red lines (bottom) are simulations on an expanded mass scale.

of the core charge trends observed for these different ionization mechanisms. The various MPCs will be referred to as unexchanged (i.e., $Au_{25}(SC2Ph)_{18}$), −SPh exchanged, −SC6 exchanged, −S−PEG−biotin exchanged, and −SPhCOOH exchanged.

Experimental Section

$Au_{25}(SC2Ph)_{18}$ MPCs were prepared following a modified Brust procedure (that was first reported[28] as giving $Au_{38}(SC2Ph)_{24}$, but later corrected[11]). The procedure used here to prepare $Au_{25}(SC2Ph)_{18}$ is exactly that reported in ref 11. Methods for preparing and purifying the thiophenolate (−SPh exchanged), hexanethiolate (−SC6 exchanged), biotinylated (−S−PEG−biotin exchanged), and 4-carboxythiophenolate (−SPhCOOH exchanged) mixed-monolayer MPC products are described in the Supporting Information.

ESI mass spectra were acquired on two instruments. The first was a Bruker BioTOF II mass spectrometer (Billerica, MA) equipped with the Apollo electrospray ionization source. (Figures 1, 2, and 4). Samples were infused at a flow rate of 65 μL/h. The ion transfer time was set to 120 μs, and 50 000 scans were averaged in the data presented. The raw data were smoothed using the Savitzky-Golay (17-point quadratic) method.[30] With the exception of LiOAc, observed clusters ($M(MOAc)_n^+$) of alkali metal acetates provided a series of convenient internal mass calibration peaks. Negative-mode calibration was performed externally using $OAc(MOAc)_n^-$ clusters. For high resolution assignments, the publicly available software, Molecular Weight Calculator,[31] was used to simulate mass spectra.

For positive-mode ESI mass spectrometry of the unexchanged material (Figure 1), $Au_{25}(SC2Ph)_{18}$ was dissolved in 1.67 mg/mL CH_2Cl_2 (or toluene). To this solution, stock methanol solutions of alkali metal acetates (MOAc), and additional methanol were added to a final composition of 70% methanol and 30% CH_2Cl_2 (or toluene). For the best results, freshly obtained, dry methanol was used (Acros 99.9%, water <50 ppm, extra dry, product number 326951000).

Positive-mode ESI mass spectra of the −SPh and −SC6 exchange products (Figure 2) were obtained using CsOAc because it provided more intense spectra than NaOAc or KOAc and did not cause additional isotopic peak broadening as RbOAc does. NaOAc was used for ESI-MS of the −S−PEG−biotin exchange product because Na^+ ions have

(30) Savitzky, A.; Golay, M. J. E. *Anal. Chem.* **1964**, *36*, 1627.
(31) Monroe, M. *Molecular Weight Calculator*. Proteomics National Center for Research Resources, Software and Tools Website. http://ncrr.pnl.gov/software/MWCalculator.stm (accessed July 16, 2007).

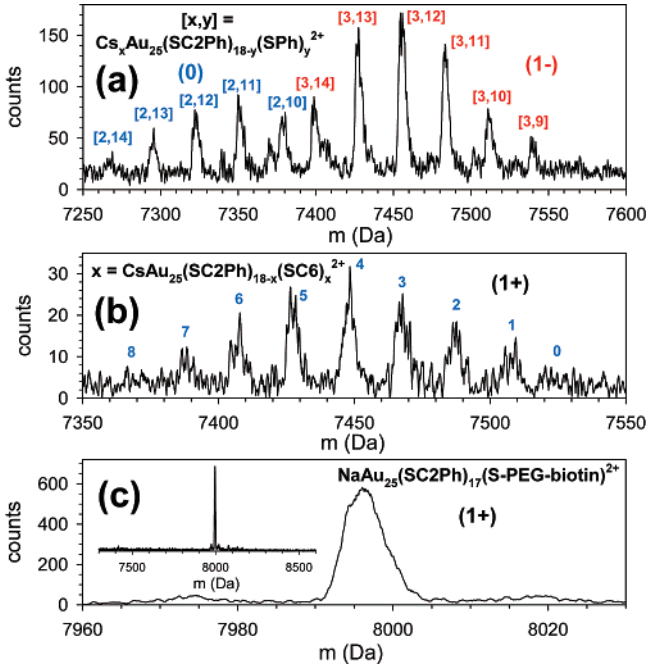

Figure 2. Mass spectra for 2+ ions of various $Au_{25}(SC2Ph)_{18}$ ligand exchange products. The core charges are indicated in parentheses: (a) HSPh exchange product with addition of 50 mmol CsOAc/1 mmol $Au_{25}(SC2Ph)_{18-y}(SPh)_y$ in 30% toluene/70% CH_3OD. (b) HSC6 exchange product with addition of 100 mmol CsOAc/1 mmol $Au_{25}(SC2Ph)_{18-x}(SC6)_x$ in 30% CH_2Cl_2/70% CH_3OH. (c) HS−PEG−biotin exchange product with addition of 50 mmol NaOAc/1 mmol $Au_{25}(SC2Ph)_{18-x}(S-PEG-biotin)_x$ in 25% toluene/75% CH_3OH.

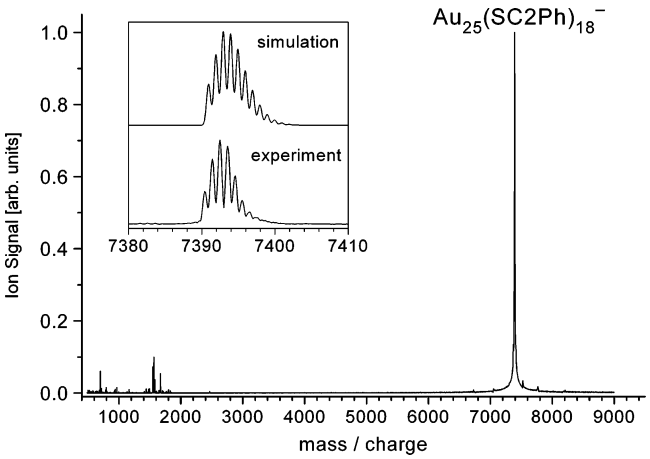

Figure 3. Negative-mode FT mass spectrum of $Au_{25}(SC2Ph)_{18}$ in 25% toluene/75% methanol. Inset: Experimentally obtained isotopomer splitting compared with a simulation for the assignment, $Au_{25}(SC2Ph)_{18}^-$ (core charge 1−).

high affinity for coordinating with PEG.[29] Each of these samples was dissolved as above for the unexchanged $Au_{25}(SC2Ph)_{18}$ material. The −SPhCOOH exchanged sample (Figure 4) was analyzed in negative mode in 100% methanol (0.50 mg/mL) using the same conditions as above.

The second instrument was a Bruker APEX II Fourier transform ion cyclotron resonance (FT-ICR) mass spectrometer equipped with an electrospray ionization source (Analytica of Branford, Branford, CT) as described in greater detail recently.[32] A negative-mode mass spectrum of $Au_{25}(SC2Ph)_{18}^-$ was acquired (Figure 3) by dissolving $Au_{25}(SC2Ph)_{18}$ (3 mg/mL) in toluene and adding methanol to a final concentration of 1 mg/mL. Typical infusion rates were 90 μL/h, and a desolvation capillary temperature of 80 °C gave the best results. For calibration,

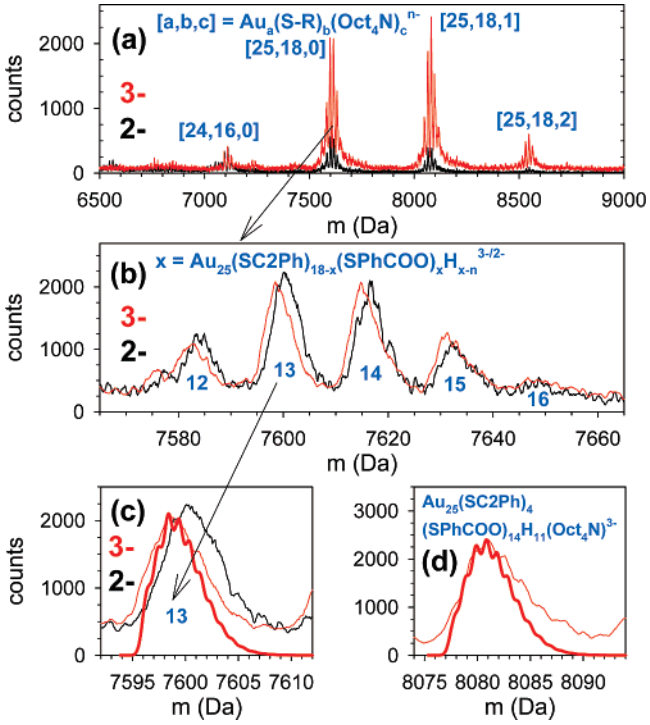

Figure 4. Mass spectra for HSPhCOOH ligand exchange products in 100% CH_3OH: (a) 3− and 2− charge states for a series of peaks that show $Au_{25}(SC2Ph)_{18-x}(SPhCOO)_xH_{x-n}^{z-}$, Oct_4N^+ binding, and the loss of Au(ligand)$_2$. The $z = 3-$ ions have core charge 1−; the 2− ions have average core charge between 0 and 1+. (b) Expansion of the set of peaks for $Au_{25}(SC2Ph)_{18-x}(SPhCOO)_xH_{x-n}^{z-}$. The data for the 2− ions are scaled up by 4×. High-resolution analysis shows an excellent match between the data (thin lines) and simulations (thick lines) for (c) $Au_{25}(SC2Ph)_5(SPhCOO)_{13}H_{11}^{3-}$ and (d) $Au_{25}(SC2Ph)_4(SPhCOO)_{14}H_{11}(Oct_4N)^{3-}$.

an aqueous solution of CsI was analyzed under virtually identical conditions and produced $(CsI)_nI^-$ ($n < 30$) clusters.

Results and Discussion

Alkali Metal Binding to Unexchanged $Au_{25}(SC2Ph)_{18}$. Mass spectra acquired under conditions as in the Experimental Section with metal acetate salts (MOAc) are not highly intense but clearly show (Figure 1) generation of cationic $M_nAu_{25}(SC2Ph)_{18}^{2+}$ species by M^+ binding. Small peaks are also seen for nanoparticles lacking M^+ binding ($0^{2+} = Au_{25}(SC2Ph)_{18}^{2+}$). We previously demonstrated that $Au_{25}(SC2Ph)_{18}$ is the unique assignment of this MPC composition;[11] it has an average mass of 7394.2 Da The peaks in Figure 1 were assigned as $z = 2+$ ions on the basis of that average mass; the 2+ charge is also consistent with the spacing between peaks corresponding to successive additions of M^+. The high-resolution data (lower part of Figure 1) for 50 mmol CsOAc: 1 mmol $Au_{25}(SC2Ph)_{18}$ in 30% toluene/70% CH_3OD show an excellent match with simulations. The assignments for these peaks are (Au core charge in parentheses): $Au_{25}(SC2Ph)_{18}^{2+}$ (2+), $CsAu_{25}(SC2Ph)_{18}^{2+}$ (1+), $Cs_2Au_{25}(SC2Ph)_{18}^{2+}$ (0), and $Cs_3Au_{25}(SC2Ph)_{18}^{2+}$ (1−).

High-resolution analyses for each of the remaining peaks that are labeled in Figure 1 and were taken with CH_2Cl_2/methanol solutions are given in the Supporting Information (Figures S-1−

(32) (a) Eichhöfer, A.; Hampe, O. *Chem. Phys. Lett.* **2005**, *407*, 186. (b) Eichhöfer, A.; Hampe, O. *Chem. Phys. Lett.* **2006**, *423*, 476. (c) Sevillano, P.; Fuhr, O.; Kattannek, M.; Nava, P.; Hampe, O.; Lebedkin, S.; Ahlrichs, R.; Fenske, D.; Kappes, M. M. *Angew. Chem., Int. Ed.* **2006**, *45*, 3702. (d) Fenske, D.; Langetepe, T.; Kappes, M. M.; Hampe, O.; Weis, P. *Angew. Chem., Int. Ed.* **2000**, *39*, 1857.

S-5), along with spectra with an expanded mass axis (Figure S-6) that show that the peaks in Figure 1 are well separated from any other peaks. Our toluene/methanol mixture spectra (Figure 1, bottom) have the best high-resolution match with the simulations, but the electrospray needle clogged frequently. Consequently, further data were acquired using the CH_2Cl_2/methanol mixture, which were consistently reproduced without clogging, but those high-resolution matches (Figures S-1−S-5) were not as uniformly good as for the toluene/methanol mixture. However, none of the data support assignments involving proton binding to the MPCs (in place of M^+ binding) in a manner that would conserve the core charge. Only through high resolution measurements such as these can the core charge be assigned unequivocally.

The ESI data taken in Na^+, K^+, Rb^+, and Cs^+ acetate solutions all show the same trend; all have ions with 0, 1, and 2 M^+ bound. The relative prominence of the 0^{2+} peak is greatest for Na^+, and for Cs^+, binding of three Cs^+ ions was also observed. In contrast, rather than binding to $Au_{25}(SC2Ph)_{18}$, Li^+ ions cause ligand loss. For the core charge assignments after ligand loss, each ligand removed was assumed to fragment as a thiolate, thereby leaving a surface Au atom with a localized positive charge. For example, after the loss of three ligands, $Au_{25}(SC2Ph)_{15}^{2+}$ has a 1− core charge in order to combine with 3+ of localized surface charges to give a 2+ ion. The specific mechanism of alkali metal cation association with $Au_{25}(SC2Ph)_{18}$ is an obvious point of interest but is not altogether clear. π−Cation interactions[33,34] with aromatic rings are well known and on electrostatic grounds are expected to be much stronger for Na^+ than Cs^+. However, the intensities of the $MAu_{25}(SC2Ph)_{18}^{2+}$ ions in Figure 1 are not very different from Na^+ to Cs^+, and a larger number of Cs^+ ions was observed to bind than Na^+, which suggests that other factors besides electrostatic-based π−cation interactions contribute. The π−cation interactions for Li^+ are expected to be the strongest of all,[34] but its binding leads to pronounced −SC2Ph ligand loss. There are two plausible contributions to ligand loss: a Li^+ ion binding to the phenyl ring may withdraw electron density and weaken the Au−S bond through an inductive effect, and/or the stability of a Li^+−thiolate cleavage product may induce Au−S bond dissociation. The former is consistent with results that both *forward and reverse* ligand exchange rates on $Au_{25}(SC2Ph)_{18}$ are faster for thiophenols with para-substituted electron-withdrawing groups, such as *p*-nitrothiophenol,[35] which implies that they are more weakly bound to the core than unsubstituted thiophenol.

We now consider the role of core electronic structure in determining the charge carried on the Au_{25} MPC core. The electron count of $Au_{25}(SC2Ph)_{18}$ is odd; therefore, a 1− or 1+ core charge would be favored in order for the HOMO (if nondegenerate) to be completely filled. Indeed, in our previous ESI-MS report[11] on the products from ligand exchange of $Au_{25}(SC2Ph)_{18}$ with HS-PEG, species such as $Na^+_{n+1}Au_{25}(SC2Ph)_{18-x}(S\text{-}PEG)_x^{n+}$ with 1− core charge were dominant in the mass spectrum. Because oxidation is the only electrochemical reaction plausibly expected in positive mode ESI, the measurement of 1− core charge suggests that the core likely had that charge in solution before its journey through the electrospray process. The charging mechanism favored in the ESI would appear to be coordination of alkali metals to the −S−PEG ligands, as opposed to core charging.

In the present results, without −S−PEG ligand exchange, charging through binding of alkali metals is considerably less efficient; the peak intensities observed in Figure 1 are smaller. It is plausible then that the variety of core charge states observed in the present case reflects an onset of charging through core oxidation. Thus, the ion counts for $Au_{25}(SC2Ph)_{18}^{2+}$ are small, while the signals for $MAu_{25}(SC2Ph)_{18}^{2+}$ with 1+ core charge are prominent. Caution is warranted, however, because a preference for a 1+ core charge might not be guided solely by the core electronic stability. Other factors, such as the MOAc concentration and the solvent system may also be significant. More information will be needed in order to further elucidate these relationships. Some general trends in the core charge are discussed further in the final section of this paper.

Monitoring Ligand Exchange and Mixed-Monolayer Compositions. ESI mass spectra of MPCs with three examples of mixed monolayers, $Au_{25}(SC2Ph)_{18-x}(SPh)_x$, $Au_{25}(SC2Ph)_{18-x}(SC6)_x$, and $Au_{25}(SC2Ph)_{17}$(S-PEG-biotin), are presented in Figure 2. ESI charging was effected using CsOAc solutions. High-resolution analyses of selected peaks are reported in the Supporting Information (Figures S-7−S-9). The extents of exchange for the different ligands are simply due to the use of different reaction times and concentrations of in-coming ligand in the exchange reactions. In Figures 2a and b, the −28 Da and −20 Da mass differences between −SC2Ph and −SPh and between −SC2Ph and −SC6, respectively, are reflected in the spacings between the adjacent major peaks in the mass spectra. The −SPh spectrum shows two sets (labeled blue and red) of overlapping peaks because binding of both two and three Cs^+ ions was observed. The ligand exchanges lead to decreases in MPC mass, while Cs^+ ion binding causes an increase; the ESI spectrum resolves both changes.

In Figure 2c, a small amount of HS−PEG−biotin was used in the exchange reaction, resulting in the exchange of only a single ligand. Due to the efficacy of Na^+/PEG coordination, an intense $NaAu_{25}(SC2Ph)_{17}(S\text{−}PEG\text{−}biotin)^{2+}$ peak was observed, which is flanked by two less intense peaks derived from the same single ligand-exchange product: $HAu_{25}(SC2Ph)_{17}(S\text{−}PEG\text{−}biotin)^{2+}$ and $Na_2Au_{25}(SC2Ph)_{17}(S\text{−}PEG\text{−}biotin)^{2+}$ (Figure S-9). For biological or medical applications of MPCs, controllable tagging with one or a small number of biological tags is often preferable in order to avoid multiple biological binding on the nanoparticle that can lead to undesired agglomeration.

These new and our previous[11] results establish ESI-MS as an effective, powerful tool for analyzing many kinds of mixed-monolayer MPCs that are prepared by ligand-exchange reactions and by other approaches. Guided by the ESI data as an analytical tool, choices of exchange times and ligand concentrations can be made that yield MPC products with desired monolayer compositions. We are currently developing a kinetic model for successive ligand exchanges with $Au_{25}(SC2Ph)_{18}$, with intent for further understanding the distribution of MPC products with different numbers of exchanged ligands.

Negative-Mode ESI-MS. The negative-ion FT mass spectrum of $Au_{25}(SC2Ph)_{18}$ shown in Figure 3 is dominated by a

(33) Dougherty, D. A. *Science* **1996**, *271*, 163.
(34) Ma, J. C.; Dougherty, D. A. *Chem. Rev.* **1997**, *97*, 1303.
(35) Guo, R.; Song, Y.; Wang, G. L.; Murray, R. W. *J. Am. Chem. Soc.* **2005**, *127*, 2752.

peak near $m/z = 7393$. The isotopomer splitting further verifies that the core charge state is indeed 1−, and the agreement with the simulated high-resolution spectrum of $Au_{25}(SC2Ph)_{18}^-$ is excellent. The experimental mass is 0.4 amu below the simulation, which is the calibration error. No higher negative charge states were observed in this mass spectrum, which indicates that this is a particularly stable charge state.

The primary mechanism of ionization in negative mode ESI-MS measurements of −SPhCOOH exchange products (Figure 4) was deprotonation. The 3− ions (red curves) gave the highest ion flux and were used for high-resolution analysis. Ions with $z = 2-$ (black curves) were also observed. The [25,18,0] = $Au_{25}(SC2Ph)_{18-x}(SPhCOO)_xH_{x-n}^{z-}$ series of peaks resembles those for −SPh and −SC6 exchanged MPC, corresponding to nanoparticles having experienced different extents of ligand exchange. Assignments and high-resolution analyses for this series of peaks are given in Figure 4b and c, and in general the matches are very good.

Additional sets of peaks were also observed at higher masses ([25,18,1] and [25,18,2]) for gas-phase adducts formed through binding of tetraoctylammonium (Oct_4N^+) to deprotonated $-SPhCOO^-$ sites in the monolayer of [25,18,0]. Oct_4N^+ was used in the original MPC synthesis; while most of these ions were removed by purification, a small amount always remains. These residual ions may be important for stabilizing the MPCs in solution, but importantly, they may be the genuine counterions of $Au_{25}(SC2Ph)_{18}^-$ MPCs having 1− core charges. Further experiments are underway to explore the utility of adduct formation (or counterion-label exchange) with other cations.

A low-intensity set of lower mass peaks in Figure 4 matches [24,16,0] = $Au_{24}(SC2Ph)_{16-x}(SPhCOO)_xH_{x-n}^{z-}$, which we believe is a fragment of [25,18,0] by loss of a gold atom and two ligands. Such core fragmentation has not been observed before in positive-mode ESI-MS. High-resolution spectra matches for peaks selected from [25,18,2], [24,16,0] and a comparison to show that [25,18,0] does not match with a hypothetical peak for Oct_4N^+ bound to [24,16,0] are presented in the Supporting Information (Figure S-10).

For $z = 3-$ ions, the predominant core charge for the [25,-18,0], [25,18,1], and [25,18,2] sets of ions is 1−, as evidenced by the high-resolution matches for $Au_{25}(SC2Ph)_5(SPhCOO)_{13}H_{11}^{3-}$, $Au_{25}(SC2Ph)_4(SPhCOO)_{14}H_{11}(Oct_4N)^{3-}$, and $Au_{25}(SC2Ph)_4(SPhCOO)_{14}H_{10}(Oct_4N)_2^{3-}$. This core charge is consistent with the observation of $Au_{25}(SC2Ph)_{18}^-$ (Figure 3) and the previous discussion that the MPCs are likely introduced from solution into the gas phase with a preexisting 1− core charge. The 2− ions are expected to be shifted to 1 Da higher mass than the 3− ions due to the presence of an additional proton. The shift is observed, but in some cases, it appears to be a 1−2 Da shift. Therefore, some ambiguity remains in the core charges of these 2− ions, but they are either 1− or 0.

These negative-mode ESI-MS results also address a potential concern about electrochemical degradation as ions are generated in an applied field during ESI.[36] In order to switch from positive mode to negative mode, the polarity of the electrospray needle potential is reversed. If the species $Au_{25}(ligand)_{18}$ were somehow a product of an electrochemical reaction followed by degradation, it would likely be observed in one mode only because the degradation products in each mode would probably differ.

Trends and Stability. In conjunction with our previous work on HS-PEG ligand-exchange products,[11] four distinct modes of ionization for $Au_{25}(ligand)_{18}$ have been observed. (1) For HS-PEG, alkali metal ions coordinate to the −S−PEG to produce predominantly 3+ and 4+ ions and a 1− core charge is usually observed; (2) for unexchanged $Au_{25}(SC2Ph)_{18}$ and the −SPh and −SC6 ligand-exchange products, less facile cation formation occurs through a combination of core oxidation and binding of alkali metal ions to produce 2+ ions; (3) direct negative-mode ionization produces $Au_{25}(ligand)_{18}^-$ ions; (4) for −SPhCOOH exchange products, 3− is the dominant ionic charge that is generated predominantly through deprotonation of −SPhCOOH, while the core has 1− or possibly 0 charge. Excluding the FT-ICR measurement (3), the efficiency of the ionization mechanisms, by ion flux counts, is: (4) ≫ (1) > (2). Negative mode is likely preferred because 1− core charge in solution favors it. Moreover, Oct_4N^+ electrosprays efficiently in positive mode,[37] which gives an ion flux that competes[38] with the MPC charging during positive-mode ESI-MS that is not present for negative mode.

These diverse ionization mechanisms show that 1− core charge is generally but not always favored. Addition of Li^+ ion to $Au_{25}(SC2Ph)_{18}$ gives some insight into the favored core charges: Loss of three ligands (1− core charge) was favored over loss of fewer ligands (0 and 1+ core charges), and no ions were observed with four or more ligands removed (2− core charge). We caution against overinterpretation of the core charges from a limited set of data, because the large field applied during ESI may induce electrochemical reactions that could distort the understanding.

Even though these measurements utilized exchanged ligands having different steric sizes, the total number of 18 ligands was conserved in every case. That indicates that the number of ligands bound is dictated by electronic considerations of the Au−S bonding, as long as steric interference between ligands is modest. It is known that the Au−S bonding also controls thiolate bonding on flat Au−thiolate self-assembled monolayers (SAMs).[39] The sharply curved average surface contour of small nanoparticle cores further disfavors steric effects as the chief consideration because more room is available for the ligand chains. However, when all of the ligands have a substantial steric bulk, it is known for slightly larger Au MPCs that the ligand space requirements can force a lower ratio of ligands to MPC core surface Au sites,[24] but we are aware of no analogous results for thiolate-proteced $Au_{25}(ligand)_{18}$.

Recent measurements by Tsukuda, et al.[5,6] have highlighted the unusual stability of $Au_{25}(SG)_{18}$, where −SG is glutathione, by demonstrating its resistance to chemical etching through addition of excess thiol and the generation of $Au_{25}(SG)_{18}$ from smaller or larger phosphine-protected Au nanoparticles. Iwasa and Nobusada have made substantial computational suggestions about the geometrical and electronic structures of differently charged $Au_{25}(SCH_3)_{18}$ species.[13] According to their computational studies, the orbitals near the Fermi level are the Au_7 core 6s and 6p orbitals: In $Au_{25}(SCH_3)_{18}^-$, the HOMO is relatively

(36) (a) Van Berkel, G. J. *J. Am. Soc. Mass Spectrom.* **2000**, *11*, 951. (b) Diehl, G.; Karst, U. *Anal. Bioanal. Chem.* **2002**, *373*, 390.

(37) Tang, L.; Kebarle, P. *Anal. Chem.* **1993**, *65*, 3654.

(38) Enke, C. G. *Anal. Chem.* **1997**, *69*, 4885.

(39) Love, J. C.; Estroff, L. A.; Kriebel, J. K.; Nuzzo, R. G.; Whitesides, G. M. *Chem. Rev.* **2005**, *105*, 1103.

high in energy and is occupied by two electrons. Because this HOMO is high in energy, electrons are readily removed to produce $Au_{25}(SCH_3)_{18}^+$, which has a low-energy HOMO and a higher ionization potential. These trends are consistent with the fact that the ESI-MS results include a preponderance of MPC core charge states 1−, 0, and 1+ but consistently fewer with 2+ cores. Moreover, because these orbitals near the Fermi level are localized on the Au_7 core, the stability of the core may dictate the stability of the whole MPC. In particular for 1− core charge, Au_7^- is a magic size, because the eight valence electrons form a closed shell in the jellium model ($1s^21p^6$).[40] The unusual stability of $Au_{25}(SG)_{18}$ has been attributed to the protection of a (−Au−S−) oligomer shell that surrounds the Au_7 core.[7,13] Tsukuda, et al. recently observed the same 1−, 0, and 1+ core charge states for $Au_{25}(SC_6H_{13})_{18}$ and noted that because each core charge state has a different electron count, the electronic structure cannot directly cause the unusual stability of $Au_{25}(ligand)_{18}$.[7] We agree that the (−Au−S−) oligomer shell is likely the source of the stability, because it geometrically restricts access to the orbitals near the Fermi level, which are localized on the Au_7 core, while still permitting electron transfer. Electronic considerations, however, must be responsible for the stability of the (−Au−S−) oligomer shell. As discussed above, the number of 18 ligands was conserved for various ligands of different steric sizes; therefore, interactions between the ligand sidechains are insufficient to give rise to the stability of the (−Au−S−) oligomer shell.

Conclusions

ESI-MS is a useful tool for the precise analysis of the core and shell composition of $Au_{25}(ligand)_{18}$ MPCs, and for mixed monolayers, it alone gives the distribution of compositions. Important information about the MPC core charge is also conveyed. Perhaps most significantly, the results show that electrospray ionization, while yielding certain predominant charged nanoparticle species, also displays a rich and varied chemistry of other events such as ligand dissociation, metal−ligand loss, and adduct formation. These details demonstrate the analytical utility of ESI-MS for nanoparticles and contribute to a deeper understanding of nanoparticle stability and reactivity. The coming challenge, of course, will be to extend these high-resolution observations of unfragmented nanoparticles to larger dimensions by eliciting higher ionization charges.

The ESI-MS method also has obvious applications for control of functionalization and biofunctionalization of nanoparticles and for study of reactions involving the core or ligand monolayer. Analysis of adduct formation, such as Oct_4N^+ binding to $-SPhCOO^-$, may provide additional insight into some kinds of MPC chemistry. These experiments also provide an important opportunity for related gas-phase spectroscopic measurements and for tandem mass spectrometry on MPCs as gas-phase ions. Such measurements could greatly enhance understanding about the structure, energetics, and reactivity of Au MPCs, in solution and in the gas phase.

Acknowledgment. We are grateful to Robert Whetten, Stefan Gilb, Manfred Kappes, Gary Glish, and Jared Bushey for helpful discussions. This research was supported in part by the National Science Foundation and Office of Naval Research. The Molecular Weight Calculator is supported by the National Institutes of Health and the Department of Energy.

Supporting Information Available: Methods for preparation and purification of ligand exchange products, high-resolution spectra and comparison with simulations for selected peaks from Figures 1, 2, and 4, mass spectra from Figure 1 with an expanded mass axis. This material is available free of charge via the Internet at http://pubs.acs.org.

JA076621A

(40) (a) Deheer, W. A. *Rev. Mod. Phys.* **1993**, *65*, 611. (b) Taylor, K. J.; Pettiette-Hall, C. L.; Cheshnovsky, O.; Smalley, R. E. *J. Chem. Phys.* **1992**, *96*, 3319.